



Published in final edited form as:

*J Biomol Screen*. 2012 September ; 17(8): 1062–1070. doi:10.1177/1087057112448100.

## Identification of Rift Valley Fever Virus Nucleocapsid Protein-RNA Binding Inhibitors Using a High-Throughput Screening Assay

Mary Ellenbecker<sup>1</sup>, Jean-Marc Lanchy<sup>1</sup>, and J. Stephen Lodmell\*

<sup>1</sup>Center for Biomolecular Structure and Dynamics, Division of Biological Sciences, The University of Montana, Missoula, MT 59812, USA.

### Abstract

Rift Valley fever virus (RVFV) is an emerging infectious pathogen that causes severe disease in humans and livestock and has the potential for global spread. Currently, there is no proven effective treatment for RVFV infection and there is no licensed vaccine. Inhibition of RNA binding to the essential viral nucleocapsid (N) protein represents a potential anti-viral therapeutic strategy because all of the functions performed by N during infection involve RNA binding. To target this interaction, we developed a fluorescence polarization-based high-throughput drug screening assay and tested 26,424 chemical compounds for their ability to disrupt an N-RNA complex. From libraries of FDA approved drugs, drug-like molecules and natural products extracts we identified several lead compounds that are promising candidates for medicinal chemistry.

### Keywords

nucleocapsid; RNA; Rift Valley fever virus; high-throughput screen; fluorescence polarization

### Introduction

Rift Valley fever virus (RVFV) is a mosquito-transmitted bunyavirus that causes disease ranging from a mild influenza-like illness to hemorrhagic fever in humans. Domestic livestock such as sheep, goats and cattle are also susceptible to RVFV infection. The mortality rate for young and newborn animals is close to 100% and the virus causes abortion in pregnant livestock<sup>2</sup>. Although historically confined to sub-Saharan Africa, RVFV has spread north to Egypt and was discovered outside of Africa for the first time in 2000. Disease symptoms can be particularly severe when the virus encounters a naïve host and outbreaks along the Nile River in Egypt and the Arabian Peninsula resulted in several devastating epidemics<sup>1;4;15;28</sup>. Global climate change, international trade and the ability of RVFV to infect a broad range of mosquito species demonstrate the possibility that RVFV will continue to disseminate geographically. Currently, treatment options for RVFV infected individuals and livestock are extremely limited. Ribavirin has been used to treat patients during past outbreaks but its use is limited due to undesirable side effects and concern related to the potential to cause birth defects<sup>3;24</sup>. T-705 (favipiravir), a promising new broad-spectrum inhibitor of viral hemorrhagic fever, is able to inhibit bunyavirus replication in experimentally infected hamsters when administered 24 hours post infection<sup>12</sup>. Studies

\*Corresponding author: J. Stephen Lodmell Tel : + (1) 406 243 6393, Fax : + (1) 406 243 4304, stephen.lodmell@umontana.edu.

<sup>1</sup>These authors contributed equally to this work.

with influenza virus showed that T-705 metabolite inhibits the viral RNA-dependent RNA polymerase<sup>9</sup>. However, the efficacy of the drug in RVFV infected humans or livestock has not yet been determined. The paucity of drugs currently licensed and available to treat viral hemorrhagic fever infection coupled with the ability of RNA viruses to mutate and develop resistance to drugs emphasize the need for continued identification of antiviral compounds.

RVFV has a tripartite single-stranded negative-sense RNA genome that encodes seven proteins. One of these gene products, the nucleocapsid (N) protein, is a 26kDa RNA binding protein that plays an important role during several stages of the viral replication cycle. N helps to package the RNA genome into the budding virus particle and regulates transcription and translation of viral mRNA and protein<sup>18;20;26</sup>. To discriminate between different species of RNA in the host cell, N recognizes and binds to specific sequences and secondary structures of viral RNA<sup>16;17</sup>. After an initial specific binding event, N switches to a non-specific mode of binding and forms polymers along the entire length of the viral genome or antigenome. This encapsidation process protects the viral RNA and prevents the formation of double stranded RNA during replication, which would activate the host anti-viral response. Inhibition of RNA binding to the essential viral nucleocapsid protein represents an attractive anti-viral therapeutic strategy because all of the functions performed by N during an infection involve RNA binding. Furthermore, significant progress has been made toward exploiting nucleocapsid protein as a drug target in HIV, respiratory syncytial virus and influenza<sup>6;11;23</sup>.

To target RNA binding activity of N, we developed a fluorescence polarization-based high-throughput drug screening (HTS) assay to test chemical compounds for their ability to disrupt an N-RNA complex *in vitro*. From libraries of FDA approved drugs, drug-like molecules, and natural product extracts, 26,424 compounds were screened and we identified 79 compounds that are inhibitors of the N-RNA interaction. We then retested the 79 hit compounds to eliminate false positives and used fluorescence polarization and filter binding assays to determine the IC<sub>50</sub> of lead compounds.

## Materials and Methods

### Compound libraries

The chemical libraries screened are a subset of either commercially available small molecule or natural product extract libraries maintained at the NERCE National Screening Laboratory (NSRB), located in the ICCB Longwood screening facility (Harvard Medical School, Boston MA). Compounds are stored desiccated at  $-20^{\circ}\text{C}$  in 384-well plates at comparable concentration of either 3.3 to 10 mM or 2 to 15 mg/ml in DMSO. Since the 23<sup>rd</sup> and 24<sup>th</sup> columns are empty for all compound plates we tested, these columns were used for screening controls.

### Fluorescent RNA aptamer to RVFV nucleocapsid N protein

The sequence of the fluorescent RNA aptamer used in the screening was obtained in our laboratory by *in vitro* selection<sup>8</sup>. Briefly, a pool of randomized RNA molecules was positively selected for efficient binding to RVFV N protein using a SELEX procedure. After 16 rounds of selection, sequencing of individual clones revealed several families of RNA aptamers. Representative clones of each family were then either terminally truncated or mutated by substitution of internal motifs. The best and smallest N aptamer resulting from these studies was the 15.12 TRNK COMP clone<sup>8</sup>. For that reason, this aptamer was chosen to be the one used during HTS. A 35 nucleotide long 15.12 TRNK COMP RNA was chemically synthesized, 3' end labeled with FAM and HPLC purified (TriLink Biotechnologies, San Diego, CA). The fluorescent label was attached to the RNA using a

six-carbon linker. The fluorescent RNA was stored at  $-80^{\circ}\text{C}$  at a concentration of  $86\ \mu\text{M}$  in water.

### Overexpression and purification of RVFV nucleocapsid N protein

The nucleocapsid N protein sequence used in this study is derived from the experimental live attenuated RVF virus vaccine strain (MP-12; <sup>5</sup>), cloned into the N-terminal (His-Asn)<sub>6</sub>-tag pEcoli plasmid (Clontech, Mountain View, CA). The N protein expression plasmid was transformed into *E. coli* strain BL21 (DE3) pLysS. Transformed cells were grown at  $37^{\circ}\text{C}$  in LB media containing  $100\ \mu\text{g/ml}$  ampicillin and  $50\ \mu\text{g/ml}$  chloramphenicol until  $\text{OD}_{600}=0.6-0.8$ . Protein expression was induced by addition of IPTG to a final concentration of  $0.5\ \text{mM}$  and cultures were grown overnight at room temperature ( $24^{\circ}\text{C}$ ). Cells were harvested by centrifugation and stored at  $-80^{\circ}\text{C}$  until processed. Eight to twelve liters of culture were processed weekly for three months. Because of the modest level of soluble protein expression, a total amount of purified N protein from 130 liters of culture was required for the screening.

Cells were lysed by resuspension of thawed pellets in Solulyse (Genlantis, San Diego, CA) lysis buffer containing a cocktail of protease inhibitors (Thermo Fisher Scientific, Waltham MA). Benzonase (EMD Chemicals, Rockland, MA) was added to the lysis buffer at a concentration of  $12\ \text{units/mL}$  to degrade nucleic acids. Insoluble cell debris was removed from the lysate by centrifugation at  $10,000\ \text{RPM}$  for 30 minutes at  $4^{\circ}\text{C}$ . The (His-Asn)<sub>6</sub>-tagged N was batch purified from the cell lysate by using  $\text{Co}^{2+}$ -charged Talon resin (Clontech). The resin was washed with 15 volumes of wash buffer ( $35\ \text{mM}$  imidazole,  $500\ \text{mM}$  NaCl,  $1\ \text{M}$  urea,  $50\ \text{mM}$  Tris-HCl pH 8.0), and the protein eluted with 4 volumes of elution buffer ( $300\ \text{mM}$  imidazole,  $500\ \text{mM}$  NaCl,  $50\ \text{mM}$  Tris-HCl pH 8.0). The eluate was dialyzed overnight against the storage buffer ( $500\ \text{mM}$  NaCl,  $10\%$  v/v glycerol,  $50\ \text{mM}$  Tris-HCl pH 8.0, two buffer changes) and concentrated using  $10\text{K}$  MWCO centrifugal filters (Amicon Millipore, Billerica, MA). After flash freezing with liquid nitrogen, the aliquots were stored at  $-80^{\circ}\text{C}$ . The purity of the protein was checked by SDS-PAGE (90%; evaluated by Coomassie staining) and the protein concentration was determined by the absorbance at  $280\ \text{nm}$  using extinction coefficient obtained from the ExpASY website ( $33,920\ \text{M}^{-1}\ \text{cm}^{-1}$ ).

### High-throughput screening

The binding of the fluorescent RNA aptamer to the RVFV N protein was monitored by fluorescence polarization. The high-throughput assay tested the ability of compounds to prevent the binding of the RNA aptamer to N (Fig. 1). Screening was performed in 384-well low volume flat bottom black microplates (Corning #3820, Corning, NY). A pilot screening (June 2011) was used to test and streamline the standard operating procedure. The frozen stocks of 10-fold binding buffer, N protein, and fluorescent RNA were sent to the screening facility ahead of time (NSRB/ICCB Longwood, Harvard Medical School, Boston MA). The optimum N protein and RNA aptamer concentrations were previously determined to be  $12\ \mu\text{M}$  and  $10\ \text{nM}$ , respectively because that resulted in a greater than 90% fractional saturation of the N-RNA complex <sup>8</sup>. The assay was further checked for HTS robustness during the pilot screening.

The main screening (August 2011) started by the thawing and pooling of all N protein aliquots. The concentration of the resulting stock was  $130\ \mu\text{M}$  (*i.e.* 11-fold concentrated) and was kept at  $4^{\circ}\text{C}$ . Each morning the amount necessary to screen the plates for the day was removed and diluted from 11- to 1.2-fold with binding buffer. The binding buffer (final concentration) is composed of  $10\ \text{mM}$  Hepes-NaOH pH 8,  $150\ \text{mM}$  NaCl,  $20\ \text{mM}$  KCl, and  $5\ \text{mM}$   $\text{MgCl}_2$ . The standard operating procedure consists of several sequential steps. First,

ten to twenty six assay plates were consecutively loaded with 10  $\mu$ l of N protein (1.2-fold in binding buffer) with a Matrix WellMate dispenser (Thermo Scientific) in all but the last (24<sup>th</sup>) column, which received 10 $\mu$ l of binding buffer. Second, 100 nl of each compound from the compound plates were transferred into the corresponding wells of the 384-well assay plates with the Epson Compound Transfer Robot. Third, two  $\mu$ l of fluorescent RNA was added to all wells of the assay plates with a Multidrop Combi nL (Thermo Fisher Scientific). After a quick centrifugation, the plates were incubated in a closed drawer at room temperature (24°C) for 30 min. Finally, the fluorescence polarization (FP) was measured with the EnVision plate reader (Perkin Elmer, Waltham, MA) and the FITC FP 480 (excitation) and 535 (emission) filters. Results were stored in Microsoft (Redmond, WA) Excel files.

### Data analysis and hit scoring

The results were transferred into a single Microsoft Excel 2011 file and analyzed using the FP, parallel and perpendicular channels values. The fluorescence polarization is defined as <sup>21</sup>:

$$FP=(I_s - I_p)/(I_s+I_p) \quad (\text{Eq. 1})$$

where FP is polarization,  $I_s$  and  $I_p$  are parallel and perpendicular polarization emission light, respectively. Practically, the FP signal is calculated as follow:

$$FP=1000*(S - G*P)/(S+G*P) \quad (\text{Eq. 2})$$

where FP is polarization in milliP (mP) units, S and P are the values of the parallel and perpendicular channels, respectively. The G-factor used during our screening was preset to 0.63. To evaluate the robustness of the assay, we quantified the Z' parameter <sup>29</sup> for each plate using the FP values of columns 23 and 24. A Z' value above 0.5 describes a suitable HTS assay <sup>29</sup>. The FP values of column 24 (RNA alone) are called positive controls, since they give the same signal than one would expect with an ideal compound, *i.e.* inhibiting 100% of protein/RNA interactions. Accordingly, FP values in column 23 (N protein and RNA) represent negative controls. Several parameters were first calculated: the sum of the fluorescence of the parallel and perpendicular channels, the average and standard deviation of positive and negative controls, the plate Z', and the amplitude of FP signal for the plate (called amplitudeFP, *i.e.* average of negative controls minus average of positive controls). Experimental wells were excluded from scoring if the sum of the parallel and perpendicular channels was lower than 10 million or greater than 20 million fluorescence units. These data allowed us to eliminate compounds that interfere with the assay detection either through quenching or compound fluorescence. The next calculation expressed the percentile of FP for an experimental well (X) related to the plate FP amplitude, provided that the well was not excluded:

$$\%FP^X=100*(FP^X - \text{average}^{\text{POS}})/\text{amplitudeFP} \quad (\text{Eq. 3})$$

where  $FP^X$  is the FP value for the well and the other parameters are described in previous paragraphs. The  $\%FP^X$  values were then filtered-in if they are below a certain percentile or filtered-out if they are above. Finally the  $\%FP^X$  for duplicates was averaged and the resulting hits were visually inspected.

### Cherry picking and final compound assessment

The protocol used during HTS was modified as followed. The final volume of the reaction in binding buffer 1x was increased from 12.1 to 24.6  $\mu$ l that includes 20  $\mu$ l of N protein at a

concentration of 14.8  $\mu\text{M}$ , 4  $\mu\text{l}$  of fluorescent aptamer RNA at 61.5 nM, and 0.6  $\mu\text{l}$  of diluted compound in DMSO 50% v/v. The cherry-picked compounds (1.2  $\mu\text{l}$  each in DMSO) were received in a 384-well plate format. A volume of 2.4  $\mu\text{l}$  DMSO 25% v/v was added to each 1.2  $\mu\text{l}$  of compound, so that 0.6  $\mu\text{l}$  of diluted compound (in DMSO 50% v/v) could be pipetted per reaction. Except for DMSO, all other molecules, including N protein, fluorescent aptamer RNA, and compound, were tested at the same concentrations than the ones used during HTS. However, we checked that the slightly higher DMSO concentration used (1.2% vs. 0.8%) did not affect fluorescence polarization (data not shown). The compounds were tested in triplicate and the results were analyzed as described above for the main HTS experiment.

### Fluorescence polarization competition assay

Fluorescence polarization competition assays were performed in 30  $\mu\text{L}$  volumes and 384-well microplate format. Samples were prepared by incubating varying concentrations of compound (8.9 nM–500  $\mu\text{M}$  final) or natural product extract ( $2.37\text{E}^{-5}$ –0.266  $\mu\text{g}/\mu\text{L}$  final) for 20 min. at room temperature ( $\sim 24^\circ\text{C}$ ) with 10  $\mu\text{M}$  N in binding buffer (10 mM HEPES-NaOH pH 8, 150 mM NaCl, 20 mM KCl, and 5 mM  $\text{MgCl}_2$ ). Next FAM-labeled aptamer RNA (10 nM final) was added and the reaction incubated for 1 hour at room temperature. Fluorescence polarization values were measured using a Biotek Synergy 2 plate reader. Excitation and emission wavelengths were 485 nm and 528 nm, respectively and the G-factor was 0.87. Binding profiles were plotted and  $\text{IC}_{50}$  values were calculated using Graph-Pad Prism software.

### Filter binding competition assay

Samples were prepared by incubating varying concentrations of compound (8.9 nM–500  $\mu\text{M}$  final) or natural product extract ( $2.37\text{E}^{-5}$ –0.266  $\mu\text{g}/\mu\text{L}$  final) for 20 min. at room temperature with 10  $\mu\text{M}$  N in binding buffer (10 mM HEPES-NaOH pH 8, 150 mM NaCl, 20 mM KCl, and 5 mM  $\text{MgCl}_2$ ). Next, 1  $\mu\text{L}$  of radiolabeled RNA ( $^{32}\text{P}$ -UTP, 25,000 cpm/ $\mu\text{L}$ ) was added to the reaction and the final volume was 12  $\mu\text{L}$ . After incubation at room temperature for one hour, reactions were diluted to 100  $\mu\text{L}$  with ice-cold binding buffer and filtered through pre-soaked nitrocellulose filters (Millipore HAWP). The filters were washed twice with 500  $\mu\text{L}$  ice-cold binding buffer, dried, and the radioactivity retained on filters was measured by scintillation counting. Binding profiles were plotted and  $\text{IC}_{50}$  values were calculated using Graph-Pad Prism software.

## Results and Discussion

### HTS assay validation

To identify compounds that could be used to develop prophylactic molecules against Rift Valley Fever Virus infection, we developed a screening assay to find inhibitors of the RVFV nucleocapsid (N) protein RNA-binding activity. Since viral RNA molecules are too large to chemically synthesize and fluorescently label we used an *in vitro* selection technique to isolate a small RNA aptamer that bound to N protein with high affinity. Competitive binding experiments using a RNA molecule that mimics the panhandle structure formed by the S segment of RVFV genomic RNA showed that the aptamer RNA binds to the same region on N as the viral panhandle<sup>8</sup>. We used fluorescence polarization (FP) to measure binding between N and a fluorescent RNA aptamer. Compounds that inhibit the protein-RNA binding decrease the FP value because the anisotropy of the free fluorescent RNA is less than that of the N-RNA complex. For instance, an ideal compound inhibiting 100% would have the same FP value than the positive control (RNA alone). During the HTS screen, the average value for the positive controls was  $158.3 \pm 8.3$  mP and the negative control average was  $282.7 \pm 10.8$  mP, resulting in an amplitude of 124.4 mP (Fig. 1).

We validated our binding assay for HTS by testing in a low volume 384-well plate format and calculating the HTS-related  $Z'$  score<sup>29</sup>. Initial experiments conducted in our own and Dr. Brian Geiss' laboratory (Colorado State University, Fort Collins, CO) showed that  $Z'$  values at or above 0.5 could be obtained (data not shown). When the experiments were done in a complete HTS environment (NSRB/ICCB Longwood, Harvard Medical School, Boston MA), the value of the pilot  $Z'$  plate was 0.51, while the plates  $Z'$  of the main screen ranged from 0.437 to 0.801. The overall  $Z'$  average of  $0.73\pm 0.052$  and the 95% confidence interval for the mean of  $0.73\pm 0.01$  underscored the validity of the assay for HTS.

### Compound screening results

The main screen was conducted over two days with 4708 and 21076 compounds tested during the first and second day, respectively. The first three series of experiments were done in duplicate. The stable and reproducible nature of the controls, as evidenced by individual plate  $Z'$  values, the reasonable number of positive hits and the rare occurrence of positive/negative pairs among duplicates (99.4% of duplicate values were 15% or less apart), as well as the limited amount of N available to work with prompted us to screen the last 52 compound plates only once in the initial screen. Compounds showing activity in this broad initial screen would be verified in follow-up assays.

Hit analysis was done for all compound well values using Microsoft Excel (see Materials & Methods) and the results are reported in Fig. 2 and Table 1. We chose a cut-off of no less than 42% inhibition (= a FP amplitude decrease of more than 58%) that led to a total of 79 hits (hit rate at 0.3%, 79/26424). The average inhibition for the hits was  $52\pm 13\%$  with a 48% median. Five of the 79 hits (6%) may be either false positive or negative: one of the two duplicate values would not have registered the compound as a hit on its own. Fifty-four of the hits belong to natural products extracts libraries (Table 1).

To validate the hits, we tested the 79 compounds and extracts in 384-well plates in our laboratory. We doubled the reaction volume and 3-fold diluted the stock of compounds we received, so a small volume of compound could be pipetted effectively. We checked that the small increase of DMSO in the final reaction had no effect on the binding yield (data not shown). The total confirmation rate was 63%, 40% for unique compounds and 74% for natural products extracts (Table 1).

Structural analysis of the 79 hit compounds revealed that four were from Life Chemicals F1860 series of aryl-benzofuran compounds. Two other molecules, Life Chemicals F0862-0529 and Chembridge 5406174, contain a quinone with an attached derivatized benzene ring (Table 2). We have yet to pursue medicinal chemistry of these compounds to determine critical features of the inhibitory mechanism.

### Dose-response studies

Cherry picked compounds that were confirmed as giving a positive result in our laboratory were purchased and the  $IC_{50}$  values for five commercially available compounds was determined using fluorescence polarization (FP). Competitive filter binding assays were also conducted to ensure that the results obtained using FP were accurate (Fig. 3). Chemical structures, results from the HTS and results from the dose-response assays for five unique compounds are summarized in Table 2. Nearly all of the compounds tested had an  $IC_{50}$  value in the low micromolar range (5–17.2  $\mu$ M). Suramin, the best inhibitor of N binding RNA in the HTS assay, is an FDA approved drug that has been used to treat trypanosomiasis. Suramin also exhibits antiretroviral activity *in vivo* by inhibiting reverse transcriptase enzymes and has been shown to have an affinity for purinergic binding sites<sup>7;13;27</sup>. These data suggest that in our system suramin prevents formation of the N-RNA

complex by interacting with the RNA binding cleft of N. Suramin is amenable to medicinal chemistry, as evidenced by the several derivatives that have been described.

The IC<sub>50</sub> value of quinacrine dihydrochloride was higher (162 μM) than the other compounds tested. Since quinacrine is known to intercalate into double-stranded DNA and structured RNA molecules, it is likely that this compound is targeting RNA itself, rather than the interaction with N protein directly<sup>19;22;25</sup>. We hypothesize that quinacrine binds to the aptamer RNA, altering its structure and thus decreasing its affinity for N. Studies conducted in picornaviruses showed that quinacrine inhibited translation of viral proteins by binding to internal ribosome entry sites in 5' untranslated region of viral mRNA<sup>10</sup>.

Two natural product extracts selected for further testing based on their performance in the HTS and follow-up assays were provided by Jon Clardy (Harvard Medical School). The IC<sub>50</sub> values of extracts 6990 and 7051 were 0.015 ng/μL and 0.030 ng/μL respectively. It is difficult to directly compare the commercially available compounds to the natural products extracts because we do not know the size or number of compounds present in an extract. As a loose approximation for discussion purposes, if we assume that the extracts contained ~20 compounds averaging ~300 Da then the IC<sub>50</sub> for the active component(s) would be in the low micromolar range (2–5 μM) and would be performing as well, or even better than the unique compounds (Table 2). We are currently seeking to identify and characterize the active component(s) in the natural product extracts that show good activity in the molecular target assay.

In conclusion, we describe a high-throughput molecular target assay that was used to identify FDA approved drugs, unique compounds and natural product extracts that have the ability to disrupt the RVFV N-RNA complex *in vitro*. Since N is indispensable for bunyavirus replication, we anticipate that a subset of the lead compounds or derivatives designed using medicinal chemistry will be efficacious in cell culture<sup>14</sup>. Specifically, we intend to test the ability of unique compounds and natural product extracts to inhibit translation of viral protein during the early stages of infection using a RVF reporter virus containing the gene for Renilla luciferase. The ability of the compounds to inhibit viral replication over the course of several days will be determined using plaque assays to quantitate production of viable virus. These secondary assays will allow us identify the compounds that have the potential to become antiviral drugs and provide us with promising candidates for future *in vivo* studies. The work presented here represents a promising start toward identifying new inhibitors of RVFV infection.

## Acknowledgments

This work was funded by the NIH/RMRCE grant AI065357 (subaward G-7826 to JSL), the Center for Biomolecular Structure and Dynamics CoBRE (Grant P20GM103546) Pilot Project award and the University Grants Program at The University of Montana.

We gratefully acknowledge Richard Elliott, Olve Peersen, and Su Chiang for helpful discussions, Brian Geiss, Doug Flood, Brian Gowen, Tao Ren for training and fruitful discussions and Jon Clardy for providing the natural product extracts.

## References

1. Balkhy HH, Memish ZA. Rift Valley fever: an uninvited zoonosis in the Arabian peninsula. *International Journal of Antimicrobial Agents*. 2003; 21:153–157. [PubMed: 12615379]
2. Bird BH, Ksiazek TG, Nichol ST, Maclachlan NJ. Rift Valley fever virus. *Journal of the American Veterinary Medical Association*. 2009; 234:883–893. [PubMed: 19335238]
3. Borio L, Inglesby T, Peters CJ, Schmaljohn AL, Hughes JM, Jahrling PB, Ksiazek T, Johnson KM, Meyerhoff A, O'Toole T, Ascher MS, Bartlett J, Breman JG, Eitzen EM Jr, Hamburg M, Hauer J,

- Henderson DA, Johnson RT, Kwik G, Layton M, Lillibridge S, Nabel GJ, Osterholm MT, Perl TM, Russell P, Tonat K. Hemorrhagic fever viruses as biological weapons. medical and public health management. *JAMA : the journal of the American Medical Association*. 2002; 287:2391–2405. [PubMed: 11988060]
4. C.D.C. Outbreak of Rift Valley fever-Saudia Arabia, August–October, 2000. *MMWR Morb Mortal Wkly Rep*. 2000; 49:905–908. [PubMed: 11043643]
  5. Caplen H, Peters CJ, Bishop DH. Mutagen-directed attenuation of Rift Valley fever virus as a method for vaccine development. *J Gen Virol*. 1985; 66 (Pt 10):2271–2277. [PubMed: 4045430]
  6. Chapman J, Abbott E, Alber DG, Baxter RC, Bithell SK, Henderson EA, Carter MC, Chambers P, Chubb A, Cockerill GS, Collins PL, Dowdell VC, Keegan SJ, Kelsey RD, Lockyer MJ, Luongo C, Najarro P, Pickles RJ, Simmonds M, Taylor D, Tyms S, Wilson LJ, Powell KL. RSV604, a novel inhibitor of respiratory syncytial virus replication. *Antimicrobial agents and chemotherapy*. 2007; 51:3346–3353. [PubMed: 17576833]
  7. De Clercq E. Suramin: a potent inhibitor of the reverse transcriptase of RNA tumor viruses. *Cancer letters*. 1979; 8:9–22. [PubMed: 92362]
  8. Ellenbecker M, Sears L, Li P, Lanchy JM, Stephen Lodmell J. Characterization of RNA aptamers directed against the nucleocapsid protein of Rift Valley fever virus. *Antiviral research*. 2012; 93:330–339. [PubMed: 22252167]
  9. Furuta Y, Takahashi K, Kuno-Maekawa M, Sangawa H, Uehara S, Kozaki K, Nomura N, Egawa H, Shiraki K. Mechanism of action of T-705 against influenza virus. *Antimicrobial agents and chemotherapy*. 2005; 49:981–986. [PubMed: 15728892]
  10. Gasparian AV, Neznanov N, Jha S, Galkin O, Moran JJ, Gudkov AV, Gurova KV, Komar AA. Inhibition of encephalomyocarditis virus and poliovirus replication by quinacrine. implications for the design and discovery of novel antiviral drugs. *Journal of virology*. 2010; 84:9390–9397. [PubMed: 20631142]
  11. Gerritz SW, Cianci C, Kim S, Pearce BC, Deminie C, Discotto L, McAuliffe B, Minassian BF, Shi S, Zhu S, Zhai W, Pendri A, Li G, Poss MA, Edavettal S, McDonnell PA, Lewis HA, Maskos K, Mortl M, Kiefersauer R, Steinbacher S, Baldwin ET, Metzler W, Bryson J, Healy MD, Philip T, Zoeckler M, Schartman R, Sinz M, Leyva-Grado VH, Hoffmann HH, Langley DR, Meanwell NA, Krystal M. Inhibition of influenza virus replication via small molecules that induce the formation of higher-order nucleoprotein oligomers. *Proceedings of the National Academy of Sciences of the United States of America*. 2011; 108:15366–15371. [PubMed: 21896751]
  12. Gowen BB, Wong MH, Jung KH, Sanders AB, Mendenhall M, Bailey KW, Furuta Y, Sidwell RW. In vitro and in vivo activities of T-705 against arenavirus and bunyavirus infections. *Antimicrobial Agents and Chemotherapy*. 2007; 51:3168–3176. [PubMed: 17606691]
  13. Kassack MU, Braun K, Ganso M, Ullmann H, Nickel P, Boing B, Muller G, Lambrecht G. Structure-activity relationships of analogues of NF449 confirm NF449 as the most potent and selective known P2X1 receptor antagonist. *European journal of medicinal chemistry*. 2004; 39:345–357. [PubMed: 15072843]
  14. Lopez N, Muller R, Prehaud C, Bouloy M. The L protein of Rift Valley fever virus can rescue viral ribonucleoproteins and transcribe synthetic genome-like RNA molecules. *Journal of virology*. 1995; 69:3972–3979. [PubMed: 7769655]
  15. Meegan JM. The Rift Valley fever epizootic in Egypt 1977–78. 1. Description of the epizootic and virological studies. *Transactions of the Royal Society of Tropical Medicine and Hygiene*. 1979; 73:618–623. [PubMed: 538803]
  16. Mir MA, Panganiban AT. The hantavirus nucleocapsid protein recognizes specific features of the viral RNA panhandle and is altered in conformation upon RNA binding. *Journal of Virology*. 2005; 79:1824–1835. [PubMed: 15650206]
  17. Mir MA, Panganiban AT. Trimeric hantavirus nucleocapsid protein binds specifically to the viral RNA panhandle. *Journal of Virology*. 2004; 78:8281–8288. [PubMed: 15254200]
  18. Mir MA, Panganiban AT. The triplet repeats of the Sin Nombre hantavirus 5' untranslated region are sufficient in cis for nucleocapsid-mediated translation initiation. *Journal of Virology*. 2010; 84:8937–8944. [PubMed: 20573811]



19. O'Brien RL, Olenick JG, Hahn FE. Reactions of quinine, chloroquine, and quinacrine with DNA and their effects on the DNA and RNA polymerase reactions. *Proceedings of the National Academy of Sciences of the United States of America*. 1966; 55:1511–1517. [PubMed: 5336287]
20. Panganiban AT, Mir MA, Bunyavirus N. eIF4F surrogate and cap-guardian. *Cell cycle*. 2009; 8:1332–1337. [PubMed: 19342890]
21. Perrin F. Polarisation de la lumière de fluorescence. Vie moyenne des molécules dans l'état excité. *J Phys Radium*. 1926; 7:390–401.
22. Pritchard NJ, Blake A, Peacocke AR. Modified intercalation model for the interaction of amino acridines and DNA. *Nature*. 1966; 212:1360–1361. [PubMed: 5967015]
23. Ramalingam D, Duclair S, Datta SA, Ellington A, Rein A, Prasad VR. RNA aptamers directed to human immunodeficiency virus type 1 Gag polyprotein bind to the matrix and nucleocapsid domains and inhibit virus production. *Journal of Virology*. 2011; 85:305–314. [PubMed: 20980522]
24. Sidwell RW, Huffman JH, Barnett BB, Pifat DY. In vitro and in vivo Phlebovirus inhibition by ribavirin. *Antimicrobial agents and chemotherapy*. 1988; 32:331–336. [PubMed: 3129991]
25. Sinha R, Hossain M, Kumar GS. RNA targeting by DNA binding drugs: structural, conformational and energetic aspects of the binding of quinacrine and DAPI to A-form and H(L)-form of poly(rC).poly(rG). *Biochimica et biophysica acta*. 2007; 1770:1636–1650. [PubMed: 17942232]
26. Strandin T, Hepojoki J, Wang H, Vaheri A, Lankinen H. The cytoplasmic tail of hantavirus Gn glycoprotein interacts with RNA. *Virology*. 2011; 418:12–20. [PubMed: 21807393]
27. Ullmann H, Meis S, Hongwiset D, Marzian C, Wiese M, Nickel P, Communi D, Boeynaems JM, Wolf C, Hausmann R, Schmalzing G, Kassack MU. Synthesis and structure-activity relationships of suramin-derived P2Y11 receptor antagonists with nanomolar potency. *Journal of medicinal chemistry*. 2005; 48:7040–7048. [PubMed: 16250663]
28. W.H.O. Rift Valley fever, Saudi Arabia (update). *Wkly Epidemiol Rec*. 2000; 75:321. [PubMed: 11050897]
29. Zhang JH, Chung TD, Oldenburg KR. A Simple Statistical Parameter for Use in Evaluation and Validation of High Throughput Screening Assays. *J Biomol Screen*. 1999; 4:67–73. [PubMed: 10838414]

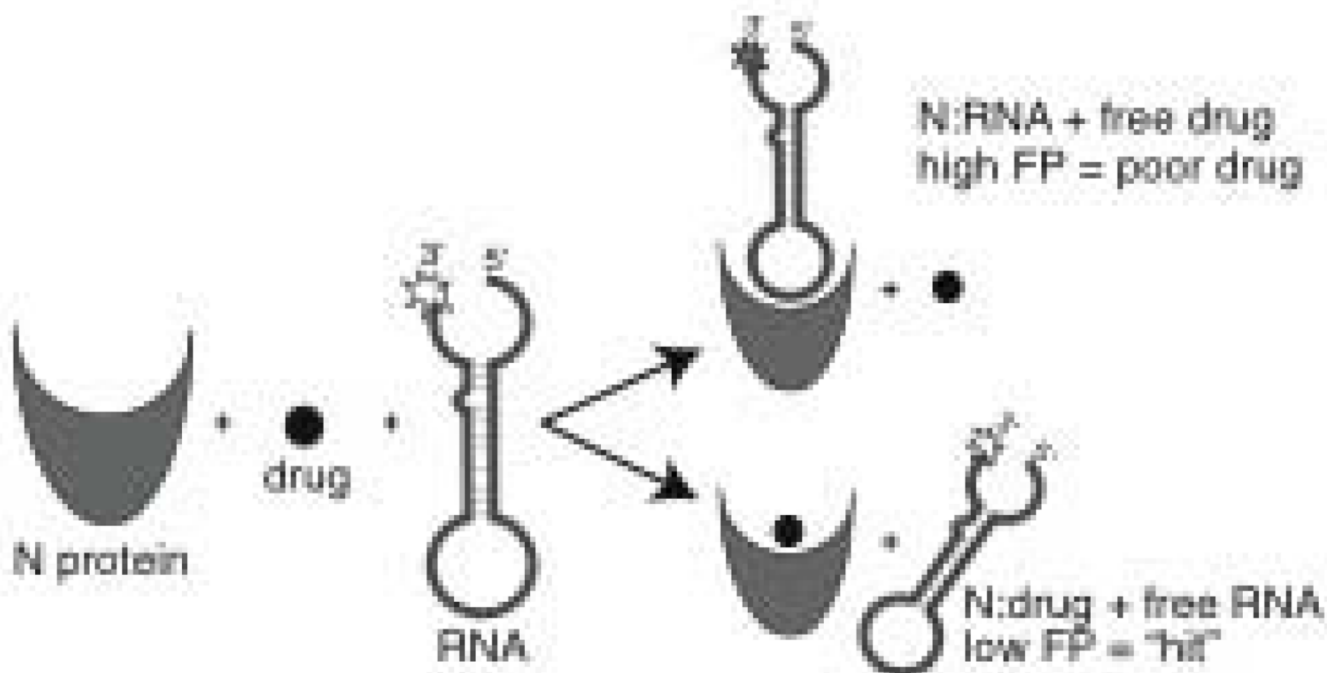


**Figure 1. High throughput screening methodology**

Schematic diagram of the technique used to identify compounds that inhibit RNA binding to N protein *in vitro*. N was loaded into 384 well microplates, drug compound was added and then fluorescently labeled RNA. After a one hour incubation, fluorescence polarization (FP) measurements were taken. A high FP signal indicates that the compound was unable to prevent the RNA from binding N protein and would not be considered a potential antiviral drug. A low FP signal is indicative of a compound that inhibits the N-RNA interaction. Experimental wells that exhibit a low FP signal are considered “hits” and the compounds in those wells could be good drug candidates. Hits identified during the initial screen are subjected to further testing and verified in follow up assays.

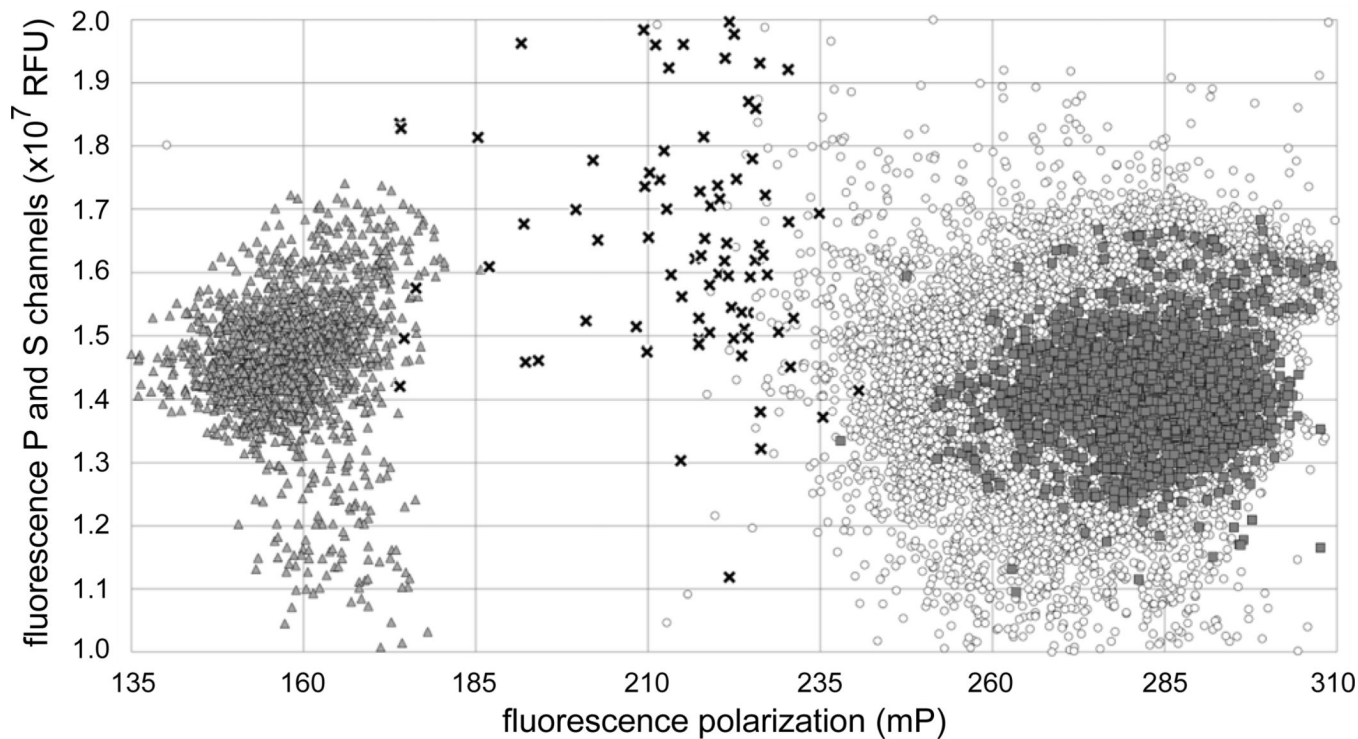


**Figure 2. Scatter plot of HTS results**

The X-axis represents the fluorescence polarization in mP units for each well. The Y-axis represents the sum of the parallel and perpendicular fluorescence channels in relative fluorescence units. The limits of the Y-axis correspond to the values used to filter in experimental values during hit analysis (between  $1-2 \times 10^7$  RFU). Positive (RNA alone) and negative (RNA and protein, no compound or extract) controls are indicated by dark triangles and dark squares, respectively. The values for the 79 hits and 26345 non-hits compounds wells are indicated by black crosses and open circles, respectively.

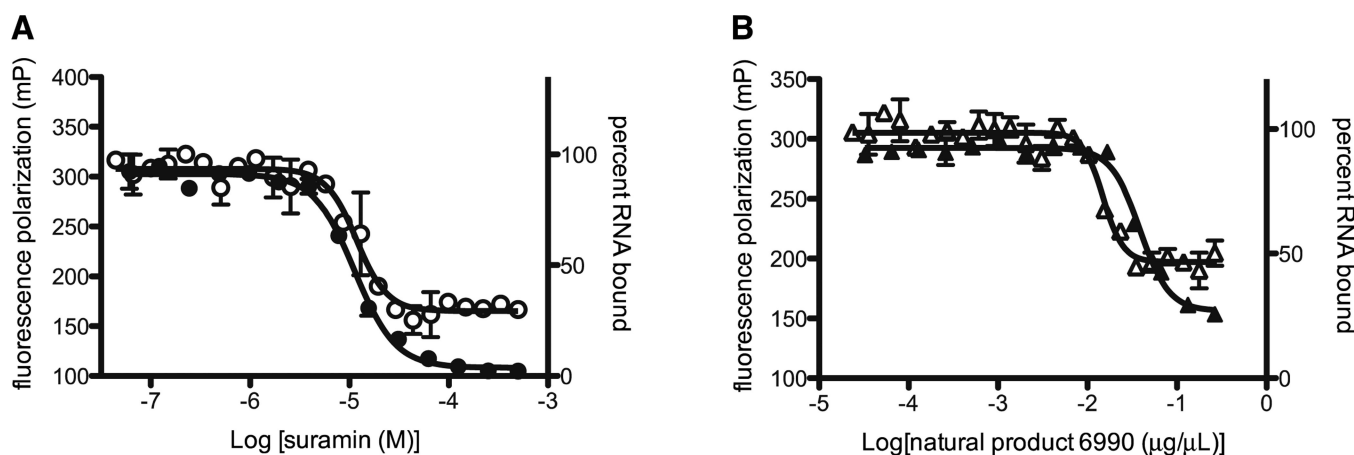


**Figure 3. Dose-response curves of suramin and natural product extract 6990**

Nitrocellulose filter binding assays (closed symbols) and fluorescence polarization (FP) (open symbols) were used to measure the ability of either suramin (A; circles) or natural product extract 6990 (B; triangles) to inhibit binding of aptamer RNA to N. The competition assays involved incubating a fixed concentration of N with varying concentrations of compound and either fluorescent or radiolabeled RNA. For the filter binding assay the amount of radiolabeled ( $^{32}\text{P}$ -UTP) aptamer RNA retained on filters was measured by liquid scintillation counting and the percent RNA bound is plotted versus compound or natural product extract concentration. The fluorescence polarization experiments used fluorescently labeled aptamer RNA and the FP signal (mP) is plotted versus compound or natural product extract concentration. The  $\text{IC}_{50}$  value calculated for suramin using a filter binding assay (A; closed circles) was  $11.3 \mu\text{M}$  and using FP (A; open circles) was  $16.3 \mu\text{M}$ . The  $\text{IC}_{50}$  value calculated for natural product extract 6990 using a filter binding assay (B; closed triangles) was  $.038 \text{ ng}/\mu\text{L}$  and using FP (B; open triangles) was  $.015 \text{ ng}/\mu\text{L}$ . Similar experiments were conducted to calculate  $\text{IC}_{50}$  values for the other unique compounds and natural product extract (Table 2). The results are the average of at least two independent experiments.

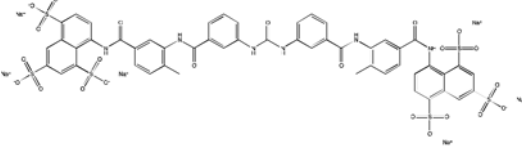
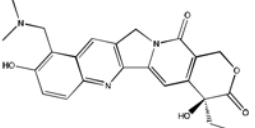
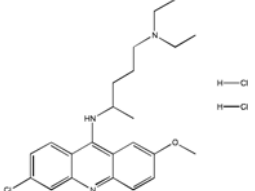
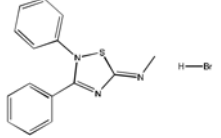
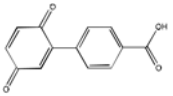
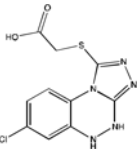
**Table 1**

Summary of statistical data from the HTS

	<b>Total</b>	<b>Unique compounds</b>	<b>Natural product extracts</b>
<b>Number of compounds screened</b>	26424	21144	5280
<b>Total hits</b>	79	25	54
<b>Overall hit rate</b>	0.3%	0.12%	1%
<b>Percent repeat</b>	63%	40%	74%
<b>Number of compounds repeated</b>	50	10	40
<b>Number of compounds tested</b>	8	6	2
<b>Average Z'</b>	0.727±0.052	0.734±0.047	0.707±0.063

Table 2

## Lead compounds and natural product extracts

Structure	Company/Library & Compound ID	Percent Inhibition HTS	IC <sub>50</sub> <sup>a</sup>	Avg. Hill slope
	Sigma Lopac suramin sodium salt	93.3	16.3±7.3 (μM)	-2.76
	BIOMOL topotecan	85.9	ND <sup>b</sup>	ND <sup>b</sup>
	BIOMOL 4 quinacrine dihydrochloride	65.7	162±26 (μM)	-2.99
	Sigma Lopac S 4063	50.3	6.7±2.9 (μM)	-1.64
	Life Chemicals 5406174	47.9	5.1±0.6 (μM)	-0.97
	Maybridge BTB 11461	44.1	17.2±3.9 (μM)	-1.27
Not applicable	ICGB Extracts 18 600 6990	72.8	0.015 ± 0.0006 (ng/μL)	-3.24
Not applicable	ICGB Extracts 18 600 7051	45.7	0.030 ± 0.0004 (ng/μL)	-0.99

<sup>a</sup>Competitive binding assays were conducted using fluorescence polarization with the exception of quinacrine which was done using a filter binding assay technique previously described in Ellenbecker et al., 2012.

ND, not determined.

<sup>b</sup>Topotecan caused protein precipitation; none of the other compounds caused obvious precipitation.